Transient Resonance Raman Investigation of the ∼570 nm Transient Absorption Band Observed after Ultraviolet Photolysis of Diiodomethane in the Solution Phase†

Yun-Liang Li, Dongqi Wang, King Hung Leung, and David Lee Phillips*

Department of Chemistry, University of Hong Kong, Pokfulam Road, Hong Kong S.A.R., P. R. China

Received: July 11, 2001; In Final Form: October 17, 2001

We present transient resonance Raman experiments done to obtain a vibrational spectrum of the photoproduct species associated with the ∼570 nm transient absorption band observed after ultraviolet photolysis of CH_2I_2 in the solution phase. The experimental vibrational frequencies and their isotopic shifts are compared to results of density functional theory calculations for the probable photoproduct species. Our results show that both the $CH_2I_2^+$ cation and *iso*-CH_2I-I species contribute to the transient ∼570 nm absorption band. The relative amounts of $CH_2I_2^+$ cation and *iso*-CH_2I-I species observed depend on the power of the 532 nm probe laser beam. We briefly discuss the qualitative properties of the visible electronic transitions of the $CH_2I_2^+$ cation and *iso*-CH_2I-I species.

Introduction

Polyhalomethanes such as CH_2I_2, CH_2BrI, and CH_2Br_2 have been measured in the troposphere and are thought to be significant sources of reactive halogens in the atmosphere.[1−6] The gas-phase ultraviolet−visible absorption spectra of CH_2I_2, CH_2BrI, and CH_2Br_2 have been obtained for the 215−390 nm region, and their atmospheric photolysis rates were estimated as a function of solar zenith angle and altitude.[5] Recently, the photolysis of CH_2I_2 and CH_2BrI in the marine boundary layer of the troposphere was linked to an increase in the concentrations of iodine oxide (IO).[7] Therefore, the photochemistry of polyhalomethanes has been of increasing interest in atmospheric chemistry. Polyhalomethanes have also been used in several synthetic chemistry reactions such as cyclopropanation of olefins and diiodomethylation of carbonyl compounds.[8−15] For example, the ultraviolet photolysis of CH_2I_2 in solutions containing olefins produces cyclopropanated products with high sterospecificity.[9,10,12]

Ultraviolet excitation (<5 eV) of gas-phase CH_2I_2 results in direct cleavage of one C−I bond to give a CH_2I radical and an iodine atom in either the ground state (I, $^2P_{3/2}$) or the spin−orbit excited state (I*, $^2P_{1/2}$).[16−18] It is energetically possible to form CH_2 and I_2 at wavelengths less than 333 nm, but this channel is symmetry-forbidden[19,20] and does not become appreciable until excitation energies are >6.4 eV.[21,22] Flash photolysis experiments have demonstrated that ultraviolet excitation of gas-phase CH_2I_2 results in mainly the CH_2I + I (or I*) products.[17] Molecular beam studies indicate the CH_2I_2 ultraviolet photodissociation takes place with a time much less than a rotational period of the parent molecule on a repulsive potential energy surface and the CH_2I photofragment gets a large degree of internal excitation of its internal degrees of freedom.[16,18,23] Infrared emission spectroscopy experiments found that the CH_2I fragment is highly vibrationally excited.[24,25] The quantum yield for formation of the I* product from the gas-phase CH_2I_2 photodissociation was also measured over the 247.5−366.5 nm range of excitation wavelengths.[19]

While the ultraviolet gas-phase CH_2I_2 reactions are reasonably well understood, the corresponding photodissociation in condensed phase environments leads to more complex photochemistry and dynamics with many conflicting reports. Ultraviolet light, direct photoionization, and radiolysis excitation of CH_2I_2 in condensed phase media all form photoproducts that have characteristic transient absorption bands ∼385 and ∼570 nm.[26−35] The identity of these photoproduct(s) has been assigned to a number of different species including trapped electrons,[26] the cation of CH_2I_2,[30,32,34] and the isomer of CH_2I_2.[28,29,35] Another assignment suggested the 385 nm absorption was due to the $CH_2I_2^+$ cation while the 570 nm band was due to the CH_2I radical.[27,31] We recently used transient resonance Raman spectroscopy experiments to directly probe the ∼385 nm transient absorption band of the product produced after ultraviolet photolysis of CH_2I_2 in cyclohexane solution.[36] Comparison of the vibrational frequencies from the transient resonance Raman experiments to those computed from density functional theory calculations for the probable photoproduct species clearly established that the isodiiodomethane (*iso*-CH_2I-I) species is mainly responsible for the characteristic ∼385 nm transient absorption band observed after condensed phase ultraviolet photolysis of CH_2I_2.[36] Further experiments using picosecond time-resolved resonance Raman spectroscopy demonstrated that the *iso*-CH_2I-I photoproduct is formed vibrationally hot within several picoseconds after photolysis.[37] Comparison of these vibrational spectroscopy results[36,37] to results previously observed in gas-phase experiments and solution phase femtosecond transient absorption experiments indicates that solvation leads to production of some *iso*-CH_2I-I product via interaction of the initially formed CH_2I and I photofragments within the solvent cage about the parent molecule.

The species responsible for the ∼570 nm transient absorption band seen after excitation of CH_2I_2 in condensed phase environments is still not clear, and the $CH_2I_2^+$ cation, CH_2I radical, and *iso*-CH_2I-I species have all been proposed in previous studies. In this paper, we report transient resonance Raman experiments that directly probe the ∼570 nm transient absorption band to obtain a vibrational spectrum of the associated photoproduct species. Comparison of the experimen-

† Part of the special issue "Mitsuo Tasumi Festschrift".

* Author to whom correspondence should be addressed.

10.1021/jp012608f CCC: $22.00
Published on Web 12/12/2001

tal vibrational frequencies and their isotopic shifts (e.g., upon changing the CH_2I_2 to a CD_2I_2 precursor) to those predicted from density functional theory calculations for the probable photoproduct species indicates that both the $CH_2I_2^+$ cation and *iso*-CH_2I-I species contribute to the transient ~570 nm absorption band. The $CH_2I_2^+$ cation and *iso*-CH_2I-I species relative contributions to the ~570 nm band depend on the power of the excitation laser beams. We briefly discuss the qualitative properties of the ~570 nm electronic transitions of the $CH_2I_2^+$ cation and *iso*-CH_2I-I species.

Experimental Procedures

CH_2I_2 (99%), CD_2I_2 (99%), and spectroscopic-grade cyclohexane (99.9%) were used to prepare samples varying in concentration from 0.20 to 0.50 M for the transient resonance Raman experiments. The apparatus and methods for the transient resonance Raman experiments have been reported previously so only a brief description will be given here.[36,38−43] The second and fourth harmonics of a nanosecond pulsed Nd:YAG laser supplied the pump (266 nm) and probe (532 nm) excitation wavelengths for the transient resonance Raman experiments. The pump and probe laser beams were lightly focused onto a flowing liquid stream of sample using a nearly collinear geometry, and an optical delay of about 0 ns was used to collect spectra. Reflective optics employing a backscattering geometry was used to collect the Raman scattered light and image it through a depolarizer and entrance slit of a 0.5 m spectrograph. The grating of the spectrograph dispersed the Raman light onto a liquid nitrogen cooled CCD detector mounted on the exit port of the spectrograph. The signal from the CCD was acquired for 300−600 s before being read out to an interfaced PC computer, and about 5−10 readouts were added together to obtain a resonance Raman spectrum. Pump-only, probe-only, and pump−probe Raman spectra as well as a background spectrum were collected, and the known Raman frequencies of the cyclohexane bands were used to calibrate the wavenumber Raman shifts of the resonance Raman spectra. The solvent and parent CH_2I_2 (or CD_2I_2) Raman bands were removed from the pump−probe transient spectrum by subtracting an appropriately scaled probe only spectrum. The pump only and background scan were also subtracted from the pump−probe spectrum.

Results and Discussion

The 266 nm pump excitation wavelength is similar to ultraviolet excitation wavelengths used in several other experiments,[26,28−30,32−36] and the 532 nm probe excitation wavelength is resonant with the blue region of the ~570 nm transient absorption band observed after photolysis of diiodomethane in condensed-phase environments.[26,28−30,32,35] Figure 1 presents transient resonance Raman spectra of CH_2I_2 in cyclohexane solution obtained with a higher-power (top) and a lower-power (bottom) 532 nm probe laser. Inspection of Figure 1 shows that the higher probe power transient resonance Raman spectrum has three large bands at 123, 488, and 575 cm^{-1} while the lower probe power has bands at 115, 123−127, 246, 488, and 575 cm^{-1}. It is interesting that the 115 and 246 cm^{-1} bands disappear in the high-power spectrum and may be due to a second photoproduct species. To better characterize these Raman bands, we have also acquired similar spectra using CD_2I_2 and examined the isotopic shifts of the transient bands. Figure 2 displays transient resonance Raman spectra of CD_2I_2 in cyclohexane solution obtained with high-power (top) and low-power (bottom) 532 nm probe laser. Examination of Figure 2 shows that the high-power spectrum has characteristic Raman bands

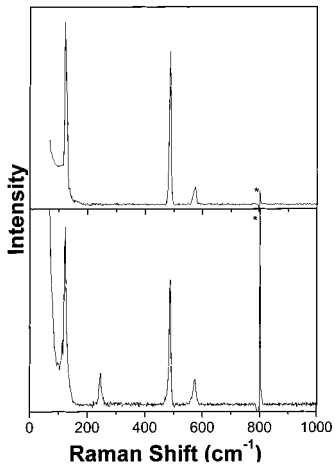

Figure 1. Transient resonance Raman spectra of the CH_2I_2 photoproduct in cyclohexane solution obtained using 266 nm pump and 532 nm probe excitation wavelengths. The top spectrum was obtained using a 532 nm probe laser energy of about 1.1 mJ/pulse. The bottom spectrum was obtained using a 532 nm probe laser energy of about 0.3 mJ/pulse. The asterisks mark solvent subtraction artifacts. The Raman shifts for the fundamental bands in the spectra are listed in Table 1. The assignments of the Raman bands are discussed in the Results and Discussion section.

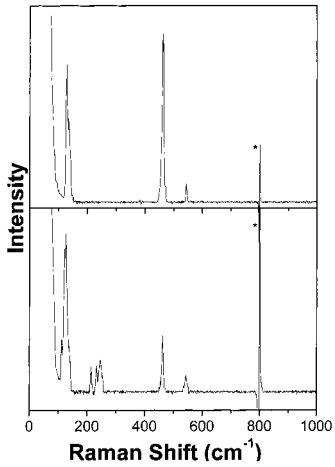

Figure 2. Transient resonance Raman spectra of the CD_2I_2 photoproduct in cyclohexane solution obtained using 266 nm pump and 532 nm probe excitation wavelengths. The top spectrum was obtained using a 532 nm probe laser energy of about 1.1 mJ/pulse. The bottom spectrum was obtained using a 532 nm probe laser energy of about 0.3 mJ/pulse. The asterisks mark solvent subtraction artifacts. The Raman shifts for the fundamental bands in the spectra are listed in Table 1. The assignments of the Raman bands are discussed in the Results and Discussion section.

at 123, 464, and 545 cm^{-1} while the low-power spectrum has characteristic bands at 113, 122, 127, 213, 233, 246, 463, and 543 cm^{-1}. The 113, 213, 233, and 246 cm^{-1} bands disappear, and the 127 cm^{-1} band is noticeably weaker in the high-power spectrum. Comparison of the transient Raman spectra in Figures 1 and 2 suggests that one species is present in the high-power spectra while two species are present in the low-power spectra.

To help identify the photoproduct species, it is useful to compare the experimental vibrational frequencies to those predicted for probable photoproduct species. We have previously done density functional theory computations to estimate the optimized geometries and vibrational frequencies for the most likely photoproduct species formed after photolysis of CH_2I_2 in condensed phases (CH_2I, $CH_2I_2^+$, and *iso*-CH_2I-I).[36] Table 1 lists the vibrational frequencies predicted from the B3LYP

TABLE 1: Comparison of the Experimental Vibrational Frequencies (in cm^{-1}) Found from the 532 nm Transient Resonance Raman Spectra (This Work), the 416 nm Transient Resonance Raman Spectra (Ref 36) and Infrared Absorption Spectra (Refs 18 and 19) to the Calculated B3LYP Density Functional Theory Vibrational Frequencies[a]

	vibrational mode	B3LYP/Sadlej TZVP (ref 36)	B3LYP/DZVP-I, TZVP-C,H (ref 36)	416 nm resonance Raman (ref 36)	532 nm resonance Raman (this work)	infrared absorption (refs 18 and 19)
			CH_2I-I (CD_2I-I)			
A′	ν_1, CH_2 sym. str.	3131 (2260) [−871]	3174 (2289) [−885]	−		3028 (2213) [−815]
	ν_2, CH_2 scissor	1340 (1011) [−329]	1384 (1037) [−347]	−		1373 (1041−1033) [−332 or −340]
	ν_3, C−I stretch	755 (645) [−110]	733 (661) [−72]	701 (640) [−61]		714/705 (645) [−69 or −60]
	ν_4, CH_2 wag	619 (476) [−143]	599 (460) [−139]	619 (496) [−123]		622−611 (498−486) [−136 to −113]
	ν_5, I−I stretch	128 (128) [0]	127 (126) [−1]	128 (128) [0]	127 (127) [0]	−
	ν_6, C−I−I bend	99 (93) [−6]	97 (92) [−5]	sh (∼110)	115 (113) [−2]	−
A″	ν_7, CH_2 asym. str.	3281 (2451) [−830]	3326 (2486) [−840]	−		3151 (2378) [−773]
	ν_8, CH_2 rock	865 (697) [−168]	888 (681) [−207]	−		−
	ν_9, CH_2 twist	447 (318) [−129]	441 (314) [−127]	487 ? (352 ?) [−135]		−
			$CH_2I_2^+$			
A_1	ν_1, CH sym. str.	3103 (2246) [−857]	3162 (2271) [−891]			
	ν_2, CH_2 def.	1365 (1003) [−362]	1414 (1031) [−383]			
	ν_3, CI sym. Str.	551 (522) [−29]	537 (511) [−26]		575 (543) [−32]	
	ν_4, ICI bend	114 (114) [0]	113 (113) [0]		123 (122) [-1]	
B_1	ν_5, CH asym. str.	3220 (2401) [−819]	3286 (2431) [−855]			
	ν_6, CH_2 rock	755 (576) [−179]	784 (597) [−187]			
A_2	ν_7, CH_2 twist	983 (696) [−287]	1003 (709) [−294]			
B_2	ν_8, CH_2 wag	1080 (813) [−267]	1120 (838) [−282]			
	ν_9, CI asym. str.	517 (490) [−27]	503 (480) [−23]		488 (463) [−25]	
			CH_2I			
A_1	ν_1, CH sym. str.	3126 (2252) [−874]	3174 (2285) [−889]			
	ν_2, CH_2 def.	1309 (974) [−335]	1353 (1006) [−347]			
	ν_3, C−I stretch	614 (576) [−38]	609 (573) [−36]			
B_1	ν_4, CH_2 wag	234 (180) [−54]	166 (129) [−37]			
B_2	ν_5, CH asym. str.	3288 (2457) [−831]	3335 (2494) [−841]			
	ν_6, CH_2 rock	832 (619) [−213]	855 (635) [−220]			

[a] The corresponding vibrational frequencies for deutrated *iso*-diiodomethane are given in parentheses. The isotopic shift of the vibrational frequency upon deuteration is given in brackets. str. = stretch; sym. = symmetric; asym. = asymmetric; def. = deformation; sh = shoulder.

calculations for the CH_2I, $CH_2I_2^+$, and *iso*-CH_2I-I species and compares them to experimental frequencies from previous 416 nm transient resonance Raman spectra[36] and infrared spectra[28,29] and our 532 nm transient resonance Raman spectra shown in Figures 1 and 2. The values in parentheses are those for the deuterated species, and the values in brackets are the isotopic frequency shifts (in cm^{-1}) found upon going from the fully protonated species to the fully deuterated species.

We shall first focus on the identity of the first species present in both the high- and low-power spectra. This species has Raman bands at 123, 488, and 575 cm^{-1} using the CH_2I_2 precursor that change to 122, 463, and 543 cm^{-1} using the CD_2I_2 precursor with isotopic shifts of about −1, −25, and −32 cm^{-1}, respectively. These experimental vibrational frequencies and isotopic shifts display reasonably good agreement with those predicted for the $CH_2I_2^+$ cation species but not the CH_2I radical or the *iso*-CH_2I-I species. For example, the CH_2I radical does not have two fundamental bands in the 400−600 cm^{-1} region, while the photoproduct species has fundamentals at 488 and 575 cm^{-1}. The 575 cm^{-1} experimental band does not correspond to an *iso*-CH_2I-I vibrational mode, and the isotopic shifts for the 575 and 488 cm^{-1} bands to 543 and 463 cm^{-1} (shifts of −32 cm^{-1} and −25 cm^{-1} respectively) do not agree with any of the *iso*-CH_2I-I modes in the 400−600 cm^{-1} region. The observed vibrational bands are assigned to the $CH_2I_2^+$ cation species as follows: the nominal C−I symmetric stretch (ν_3) is assigned to the 575 cm^{-1} experimental band, the nominal ICI bend (ν_4) is assigned to the 123 cm^{-1} experimental band, and the CI asymmetric stretch (ν_9) is assigned to the 488 cm^{-1} experimental band.

The second species present in the low-power probe spectra appears to have bands at 113 and 246 cm^{-1} in the transient spectrum after photolysis of CH_2I_2. The 246 cm^{-1} band can be either a fundamental or an overtone of the intense ∼123−127 cm^{-1} fundamental band in the transient Raman spectra of Figure 1. The low-power CD_2I_2 transient resonance Raman spectrum displays several bands at 113, 213, 233, and 246 cm^{-1} that are not present in the high-power probe transient resonance Raman spectrum. In addition, the ∼123−127 cm^{-1} band in the low-power probe transient resonance Raman spectra in Figures 1 and 2 appears somewhat more intense relative to the 488 cm^{-1} band of the $CH_2I_2^+$ cation species. This suggests the second photoproduct species may also have a low-frequency mode in the 123−127 cm^{-1} region. If this is the case, then the second photoproduct species has two low-frequency modes at 113 and ∼123−127 cm^{-1}, respectively. The 246 cm^{-1} mode in Figure 1 (bottom) could be assigned to the overtone of the intense ∼123−127 cm^{-1} fundamental. The 213, 233, and 246 cm^{-1} modes in Figure 2 could then be assigned to the overtone of the 113 cm^{-1} band, the combination band of 113 and ∼123−127 cm^{-1} fundamentals, and the overtone of the ∼123−127 cm^{-1} fundamental, respectively. Of the three probable photoproduct species ($CH_2I_2^+$, CH_2I, and *iso*-CH_2I-I), only *iso*-CH_2I-I has two low-frequency modes below 200 cm^{-1} (see Table 1). These two low-frequency modes whose fundamentals are observed at 115 cm^{-1} (113 cm^{-1} for fully deuterated species) and ∼127 cm^{-1} have overtones and combination bands that could account for the experimental Raman bands observed at 213, 233, and 246 cm^{-1} in the low-power probe CD_2I_2 transient Raman spectrum (bottom of Figure 2). We therefore assign *iso*-

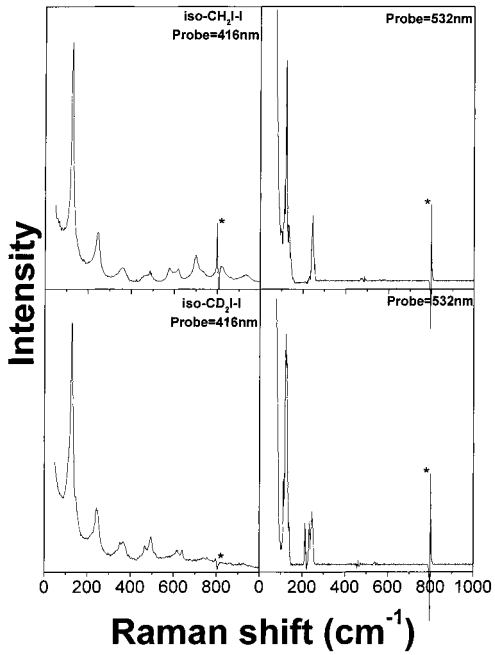

Figure 3. Transient resonance Raman spectra of the CH_2I_2 (top) and CD_2I_2 (bottom) photoproducts in cyclohexane solution obtained using 309 nm pump and 416 nm probe wavelengths (left) and using 266 nm pump and 532 nm probe excitation wavelengths (right). The top and bottom right spectra (using a 532 nm probe laser) were obtained by subtracting an appropriately scaled high-power spectrum from a low-power spectrum (shown in Figures 1 and 2 for excitation of CH_2I_2 and CD_2I_2 respectively) to remove the bands due to the cation species. The asterisks mark solvent subtraction artifacts. The Raman shifts for the fundamental bands in the spectra are listed in Table 1. The assignments of the Raman bands are discussed in the Results and Discussion section.

CH_2I-I to the second photoproduct species observed using low-power probe laser excitation. The band in the 123−127 cm^{-1} region is assigned to the fundamental of the nominal I−I stretch mode (ν_5), and the 115 cm^{-1} band is assigned to the fundamental of the nominal C−I−I bend mode (ν_6) of the *iso*-CH_2I-I species.

Figure 3 compares 532 nm probe transient resonance Raman difference spectra (low-power−high-power spectra shown in Figures 1 and 2) to spectra previously obtained with 416 nm excitation (resonant with the ∼385 nm transient absorption band) and assigned to the *iso*-CH_2I-I species.[36] Inspection of Figure 3 reveals that the predominant progression for the *iso*-CH_2I-I species in the 416 nm transient resonance Raman spectra is the $n\nu_5$ nominal I−I stretch progression and its combination bands with the nominal C−I−I bend mode (ν_6). Upon going from the *iso*-CH_2I-I species to the *iso*-CD_2I-I species, the ν_6 mode and its combination bands with the nominal I−I stretch mode (ν_5) become more apparent in the 416 nm transient resonance Raman spectra.[36] This behavior is very similar to that observed for the second photoproduct species in the 532 nm transient resonance Raman difference spectra (upon going from CH_2I_2 to CD_2I_2 precursor) in Figure 3 and consistent with our assignment of the second photoproduct species to *iso*-CH_2I-I.

Why do the resonance Raman bands associated with the *iso*-CH_2I-I species disappear when a high-power probe 532 nm laser excitation is used (see Figures 1 and 2)? Maier and coworkers noted that further ultraviolet or visible excitation of the transient absorption bands formed after ultraviolet photolysis of CH_2I_2 in low-temperature matrixes leads to almost quantitative reformation of the parent diiodomethane (CH_2I_2) molecule.[28,29] This is similar to what we observed for the disappearance of the *iso*-CH_2I-I Raman bands as the 532 nm probe laser power is increased. The *iso*-CH_2I-I species is prone to undergo a secondary photochemical reaction, and it is likely that the very weak I−I bond in *iso*-CH_2I-I photodissociates to give CH_2I and I fragments that can recombine to reform the parent CH_2I_2 molecule in significant amounts. This would be consistent with the relative intensity pattern of the *iso*-CH_2I-I transient resonance Raman bands which have most of their intensity in the I−I stretch overtone progression ($n\nu_5$) and its combination bands with other Franck−Condon active modes. The relative resonance Raman intensity pattern for the *iso*-CH_2I-I spectra shown in Figure 3 is very similar to resonance Raman spectra of alkyl iodides and dihalomethanes associated with A-band electronic transitions known to lead to direct C−I bond photodissociation have most of their intensity in the nominal C−I stretch overtone progression and its combination bands with other Franck−Condon active modes.[44−59] The large intensity in the overtones of the I−I stretch in *iso*-CH_2I-I and the C−I stretch overtones in the alkyl iodides and dihalomethanes indicates a very large change in the bond length and bond order in these modes consistent with their direct photodissociation. In contrast, the resonance Raman spectra for the $CH_2I_2^+$ cation in Figures 1 and 2 display very little intensity in their overtones or combination bands. This indicates that the excited state of the $CH_2I_2^+$ cation does not experience much change in the bond lengths or bond order of the nominal C−I symmetric stretch, the nominal ICI bend, and the CI asymmetric stretch modes. Thus, further excitation of *iso*-CH_2I-I with 532 nm light appears to result in photodissociation of the I−I bond, while similar excitation of the $CH_2I_2^+$ cation does not photodissociate the stronger C−I bond. This is consistent with the probe power dependence of the 532 nm transient resonance Raman spectra shown in Figures 1 and 2.

The C−I bond in the $CH_2I_2^+$ cation is somewhat stronger (575 cm^{-1}) than those in typical alkyl iodides (480−530 cm^{-1}) which require at least near-ultraviolet excitation to photodissociate the C−I bond. Therefore, one would expect that 532 nm light would not have enough energy to dissociate the C−I bond of the $CH_2I_2^+$ cation. The I−I bond in *iso*-CH_2I-I is weaker (127 cm^{-1}) compared to an iodine bond (∼210 cm^{-1}) which can be photodisociated by 532 nm excitation.[60−76] Thus, one would reasonably expect the I−I bond to photodissociate upon 532 nm excitation of the I−I chromophore in the *iso*-CH_2I-I species. The probe power dependence of the 532 nm transient resonance Raman spectra shown in Figures 1 and 2, and the relative resonance Raman intensity patterns of the $CH_2I_2^+$ cation and *iso*-CH_2I-I species are consistent with the preceding expectations.

Our present results indicate that ultraviolet excitation of CH_2I_2 in liquids using a moderately focused laser beam leads to formation of *iso*-CH_2I-I species (via solvent-induced recombination of the CH_2I and I fragments)[35−37] and some $CH_2I_2^+$ cation species (likely via two-photon ionization). The branching ratio for these two channels probably depends noticeably on the type of excitation of CH_2I_2 in condensed-phase environments. For example, pulse radiolysis may be expected to produce more photoionization relative to fragmentation, while low-power ultraviolet excitation may be expected to produce more fragmentation compared to photoionization. The ∼570 nm transient absorption band has noticeable contributions from both $CH_2I_2^+$ cation and *iso*-CH_2I-I species, while the ∼385 nm transient absorption band appears to be mainly associated with the *iso*-CH_2I-I species.[36,37] If more $CH_2I_2^+$ cation species are formed relative to the *iso*-CH_2I-I species, one could reasonably expect that the ∼570 nm absorption band may increase in intensity

relative to the ~385 nm transient absorption band. There is some evidence in the literature that this may indeed be the case. Ultraviolet excitation of CH_2I_2 leads to formation of the ultraviolet and visible transient absorption bands with an intensity ratio of about 5.6 to 1 (see Figure 2 of ref 28). However, pulsed radiolysis leads to formation of these two bands with an intensity ratio of about 3:1 (see Figure 7 of ref 32). This apparent increase in the visible transient absorption band intensity relative to the ultraviolet transient absorption band using pulsed radiolysis compared to low-power ultraviolet excitation is consistent with the hypothesis that pulse radiolysis results in more photoionization compared to fragmentation relative to low-power ultraviolet excitation. However, more work is needed to elucidate why the ultraviolet and visible transient absorption bands intensity changes as a function of type of excitation. At this time, it is not clear what the branching ratios and quantum yields are for formation of the *iso*-CH_2I-I, CH_2I, and $CH_2I_2^+$ cation photoproducts as the type of excitation is changed, the excitation energy is changed, and the solvent environment is changed. More experimental and theoretical work is needed to address these issues. Our present work indicates that time-resolved resonance Raman spectroscopy can conveniently be used to clearly distinguish the relative contributions of the *iso*-CH_2I-I and $CH_2I_2^+$ cation photoproducts to the ~570 nm transient absorption band. The resonance Raman experiments requires the use of a focused laser beam. An experimental difficulty in obtaining an excitation profile is the need to account for any changes in the photon flux in the sample area of excitation as the probe wavelength is varied (due to changes in index of refraction, pulse to pulse variations, power drift, and/or sample degradation). Similarly, investigation of solvent effects on the branching ratio between formation of the *iso*-CH_2I-I and $CH_2I_2^+$ cation species would also require some knowledge of how the intensity and band-shape of the transient absorption changes as a function of solvent. We plan to explore solvent effects and possibly some wavelength-dependent behavior in the future.

Acknowledgment. D.L.P. would like to thank the Committee on Research and Conference Grants (CRCG) and the Research Grants Council of Hong Kong (HKU 7087/01P) for support of this research.

References and Notes

(1) Class, Th.; Ballschmiter, K. *J. Atmos. Chem.* **1988**, *6*, 35.
(2) Klick, S.; Abrahamsson, K. *J. Geophys. Res.* **1992**, *97*, 12683.
(3) Heumann, K. G. *Anal. Chim. Acta* **1993**, *283*, 230.
(4) Moore, R. M.; Webb, M..; Tokarczyk, R.; Wever, R. *J. Geophys. Res.-Oceans* **1996**, *101* (C9), 20899.
(5) Mössigner, J. C.; Shallcross, D. E.; Cox, R. A. *J. Chem. Soc., Faraday Trans.* **1998**, *94*, 1391.
(6) Carpenter, L. J.; Sturges, W. T.; Penkett, S. A.; Liss, P. S. *J. Geophys. Res.-Atmos* **1999**, 104, 1679.
(7) Alicke, B.; Hebstreit, K.; Stutz, J.; Platt, U. *Nature 1999*, 397, 572.
(8) Simmons, H. E.; Smith, R. D. *J. Am. Chem. Soc.* **1959**, *81*, 4256.
(9) Blomstrom, D. C.; Herbig, K.; Simmons, H. E. *J. Org. Chem.* **1965**, *30*, 959.
(10) Pienta, N. J.; Kropp, P. J. *J. Am. Chem. Soc.* **1978**, *100*, 655.
(11) Kropp, P. J.; Pienta, N. J.; Sawyer, J. A.; Polniaszek, R. P. *Tetrahedron* **1981**, *37*, 3229.
(12) Kropp, P. J. *Acc. Chem. Res.* **1984**, *17*, 131.
(13) Friedrich, E. C.; Lunetta, S. E.; Lewis, E. J. *J. Org. Chem.* **1989**, *54*, 2388.
(14) Durandetti, S.; Sibille, S.; Pérchon, J. *J. Org. Chem.* **1991**, *56*, 3255.
(15) Concellón, J. M.; Bernad, P. L.; Pérez-Andrés, J. A. *Tetrahedron Lett.* **1998**, *39*, 1409.
(16) Kawasaki, M.; Lee, S. J.; Bersohn, R. *J. Chem. Phys.* **1975**, *63*, 809.
(17) Schmitt, G.; Comes, F. J. *J. Photochem.* **1980**, *14*, 107.
(18) Kroger, P. M.; Demou, P. C.; Riley, S. J. *J. Chem. Phys.* **1976**, *65*, 1823.
(19) Koffend, J. B.; Leone, S. R. *Chem. Phys. Lett.* **1981**, *81*, 136.
(20) Cain, S. R.; Hoffman, R.; Grant, R. *J. Phys. Chem.* **1981**, *85*, 4046.
(21) Marvet, U.; Dantus, M. *Chem. Phys. Lett.* **1996**, *256*, 57.
(22) Zhang, Q.; Marvet, U.; Dantus, M. *J. Chem. Phys.* **1998**, *109*, 4428.
(23) Jung, K.-W.; Ahmadi, T. S.; El-Sayed, M. A. *Bull. Korean Chem. Soc.* **1997**, *18*, 1274.
(24) Baughcum, S. L.; Hafmann, H.; Leone, S. R.; Nesbitt, D. *J. Faraday Discuss. Chem. Soc.* **1979**, *67*, 306.
(25) Baughcum, S. L.; Leone, S. R. *J. Chem. Phys.* **1980**, *72*, 6531.
(26) Simons, J. P.; Tatham, P. E. R. *J. Chem. Soc. A* **1966**, 854.
(27) Mohan, H.; Rao, K. N.; Iyer, R. M. *Radiat. Phys. Chem.* **1984**, *23*, 505.
(28) Maier, G.; Reisenauer, H. P. *Angew. Chem., Int. Ed. Engl.* **1986**, *25*, 819.
(29) Maier, G.; Reisennauer, H. P.; Hu, J.; Schaad, L. J.; Hess, B. A., Jr. *J. Am. Chem. Soc.* **1990**, *112*, 5117.
(30) Andrews, L.; Prochaska, F. T.; Ault, B. S. *J. Am. Chem. Soc.* **1979**, *101*, 9.
(31) Mohan, H.; Iyer, R. M. *Radiat. Eff.* **1978**, *39*, 97.
(32) Mohan, H.; Moorthy, P. N.; *J. Chem. Soc., Perkin Trans. 2* **1990**, 277.
(33) Schwartz, B. J.; King, J. C.; Zhang, J. Z.; Harris, C. B. *Chem. Phys. Lett.* **1993**, *203*, 503.
(34) Saitow, K.; Naitoh, Y.; Tominaga, K.; Yoshihara, K. *Chem. Phys. Lett.* **1996**, *262*, 621.
(35) Tarnovsky, A. N.; Alvarez, J.-L.; Yartsev, A. P.; Sundström, V.; Åkesson, E. *Chem. Phys. Lett.* **1999**, *312*, 121.
(36) Zheng, X.; Phillips, D. L. *J. Phys. Chem. A* **2000**, *104*, 6880.
(37) Kwok, W. M.; Ma, C.; Parker, A. W.; Phillips, D.; Towrie, M.; Matousek, P.; Phillips, D. L. *J. Chem. Phys.* **2000**, *113*, 7471.
(38) Pan, D.; Shoute, L. C. T.; Phillips, D. L. *J. Phys. Chem. A* **1999**, *103*, 6851.
(39) Zheng, X.; Phillips, D. L. *Chem. Phys. Lett.* **2000**, *324*, 175.
(40) Zheng, X.; Phillips, D. L. *J. Chem. Phys.* **2000**, *113*, 3194.
(41) Zheng, X.; Kwok, W. M.; Phillips, D. L. *J. Phys. Chem. A* **2000**, *104*, 10464.
(42) Zheng, X.; Fang, W.-H.; Phillips, D. L. *J. Chem. Phys.* **2000**, *113*, 10934.
(43) Zheng, X.; Lee, C. W.; Li, Y.-L.; Fang, W.-H.; Phillips, D. L. *J. Chem. Phys.* **2001**, *114*, 8347.
(44) Zhang, J.; Imre, D. G. *J. Chem. Phys.* **1988**, *89*, 309.
(45) Lao, K. Q.; Person, M. D.; Xayaroboun, P.; Butler, L. J. *J. Chem. Phys.* **1990**, *92*, 823.
(46) Galica, G. E.; Johnson, B. R.; Kinsey, J. L.; Hale, M. O. *J. Phys. Chem.* **1991**, *95*, 7994.
(47) Phillips, D. L.; Lawrence, B. A.; Valentini, J. J. *J. Phys. Chem.* **1991**, *95*, 9085.
(48) Phillips, D. L.; Myers, A. B. *J. Chem. Phys.* **1991**, *95*, 226.
(49) Phillips, D. L.; Valentini, J. J.; Myers, A. B. *J. Phys. Chem.* **1992**, *96*, 2039.
(50) Wang, P. G.; Ziegler, L. D. *J. Phys. Chem.* **1993**, *97*, 3139.
(51) Markel, F.; Myers, A. B. J. *Chem. Phys.* **1993**, *98*, 21.
(52) Kwok, W. M.; Phillips, D. L. *Chem. Phys. Lett.* **1995**, *235*, 260.
(53) Man, S. Q.; Kwok, W. M.; Phillips, D. L. *J. Phys. Chem.* **1995**, *99*, 15705.
(54) Kwok, W. M.; Phillips, D. L. *J. Chem. Phys.* **1996**, *104*, 2529.
(55) Kwok, W. M.; Phillips, D. L. *J. Chem. Phys.* **1996**, *104*, 9816.
(56) Man, S. Q.; Kwok, W. M.; Johnson, A. E.; Phillips, D. L. *J. Chem. Phys.* **1996**, 105, 5842.
(57) Duschek, F.; Schmitt, M.; Vogt, P.; Materny, A.; Kiefer, W. *J. Raman Spectrosc.* **1997**, *28*, 445.
(58) Braun, M.; Materny, A.; Schmitt, M.; Kiefer, W.; Engel, V. *Chem. Phys. Lett.* **1998**, *284*, 39.
(59) Phillips, D. L. *Prog. React. Kinet. Mech.* **1999**, *24*, 223.
(60) Chuang, T. J.; Hoffman, G. W.; Eisenthal, K. B. *Chem. Phys. Lett.* **1974**, *25*, 201.
(61) Harris, A. L.; Brown, J. K.; Harris, C. B. *Annu. Rev. Phys. Chem.* **1988**, *39*, 341.
(62) Scherer, N. F.; Jonas, D. M.; Fleming, G. R. *J. Chem. Phys.* **1993**, *99*, 153.
(63) Zadoyan, R.; Sterling, M.; Ovchinnokov, M.; Apkarian, V. A. *J. Chem. Phys.* **1997**, *107*, 8446.
(64) Liu, Q.; Wang, J.-K.; Zewail, A. H. *Nature* **1993**, *364*, 427.
(65) Wang, J.-K.; Liu, Q.; Zewail, A. H. *J. Phys. Chem.* **1995**, *99*, 11309.
(66) Schroeder, J.; Troe, J.; *Annu. Rev. Phys. Chem.* **1987**, *38*, 163.
(67) Lienaum, Ch.; Williamson, J. C.; Zewail, A. H. *Chem. Phys. Lett.* **1993**, *213*, 289.
(68) Zadoyan, R.; Sterling, M.; Apkarian, V. A. *J. Chem. Soc., Faraday Trans.* **1996**, *92*, 1821.

(69) Zadoyan, R.; Almy, J.; Apkarian, V. A. *J. Faraday Discuss.* **1997**, *108*, 255.
(70) Bardeen, C. J.; Che, J.; Wilson, K. R.; Yakovlev, V. V.; Apkarian, V. A.; Martens, C. C.; Zadoyan, R.; Kohler, B.; Messina, M. *J. Chem. Phys.* **1997**, *106*, 8486.
(71) Andrews, L. *Appl. Spectrosc. Rev.* **1976**, *11*, 125.
(72) Sension, R. J.; Strauss, H. L. *J. Chem. Phys.* **1986**, *85*, 3791.
(73) Sension, R. J.; Kobayashi, T.; Strauss, H. L. *J. Chem. Phys.* **1987**, *87*, 6221.
(74) Sension, R. J.; Strauss, H. L. *J. Chem. Phys.* **1988**, *88*, 2289.
(75) Xu, J.; Schwenter, N.; Chergui, M. *J. Chem. Phys.* **1994**, *101*, 7381.
(76) Xu, J.; Schwenter, N.; Hennig, S.; Chergui, M. *J. Raman Spectrosc.* **1997**, *28*, 433.